

# Photoinduced Floquet topological magnons in a ferromagnetic checkerboard lattice

Zhiqin Zhang<sup>1,a</sup>, Wenhui Feng<sup>1,a</sup>, Yingbo Yao<sup>3</sup>, Bing Tang<sup>1,2\*</sup>

<sup>1</sup> *Department of Physics, Jishou University, Jishou 416000, China*

<sup>2</sup> *The Collaborative Innovation Center of Manganese-Zinc-Vanadium Industrial Technology, Jishou University, Jishou 416000, China*

<sup>3</sup> *College of Information and Electronic Engineering, Hunan City University, Yiyang 413000, China*

*Keywords:* Floquet topological magnons; Topological phase transitions; The Floquet-Bloch theory; Irradiated checkerboard ferromagnets

## ABSTRACT

Since the magnon is an uncharged bosonic quasiparticle carrying the magnetic dipole moment, the topological magnon insulators can interact with the electromagnetic (laser) field by the Aharonov-Casher effect. This theoretical work is devoted to investigating laser-irradiated Floquet topological magnon insulators on a two-dimensional checkerboard ferromagnet and their topological phase transitions. With the help of the Floquet-Bloch theory, we find that the checkerboard Floquet topological magnon insulators can be transformed from one topological magnon insulator into another one with various Berry curvatures and Chern numbers by changing the light intensity. Furthermore, the thermal Hall effect in the checkerboard Floquet topological magnon insulator are also discussed.

\* Corresponding author.

E-mail addresses: [bingtangphy@jsu.edu.cn](mailto:bingtangphy@jsu.edu.cn)

<sup>a</sup> These authors contributed equally to this work.

## 1. Introduction

Up to now, topological insulators have received more and more attention from the theoretical and experimental researchers[1]. Such nontrivial insulators have been realized in electronic systems, which possess a bulk band gap like a common insulator but possess the topologically protected edge states due to the bulk-boundary correspondence[2]. Theoretically, the notion of the topological band structure does not rely on the statistical property of the quasiparticle excitations. On the other hand, the notion of Chern number and Berry curvature can be given for any topological energy band structure without respect to the quasiparticle excitations. Naturally, these topological concepts can be expanded to bosonic systems such as photons[3], phonons[4], and magnons[5].

In recent years, there has been an increasing interest in studies on the topological magnon insulator, which can be viewed as the bosonic counterpart of the topological insulator in electronic systems. Topological magnon insulators have nontrivial magnon energy bands and topologically protected magnon edge states. Initially, Onose *et al.* have discovered the magnon Hall effect in the insulating ferromagnet  $\text{Lu}_2\text{V}_2\text{O}_7$  with pyrochlore lattice[6]. Their result have showed a transverse heat current upon application of a longitudinal temperature gradient. Immediately, Matsumoto and Murakami have explained that the emergence of the magnon Hall effect is due to magnon edge currents in the two-dimensional quantum magnetic systems[7,8]. Later on, Zhang *et al.* [9] have taken cognizance of that this magnon edge current is caused by the nontrivial band topology of quantum ferromagnets, and realized topological magnon insulators for the first time. Physically, topological magnetic excitations can appear in topological quantum magnets with various lattice geometries, however it is very hard to experimentally observe real magnetic materials them. So far, the intrinsic topological magnon insulator has been observed experimentally in a quasi-2D kagomé ferromagnet  $\text{Cu}(1-3, \text{ bdc})$  [10]. Furthermore, topological magnons have also been investigated in ferromagnets with other lattice structures, such as the honeycomb[11], Lieb[12], star[13], checkerboard[14], and Shastry-Sutherland lattices[15].

In principle, those charge-neutral magnons in the insulating quantum magnet can be regarded as the magnetic dipole moments hopping on lattices[16]. A magnetic dipole moving in the external electric field accumulates a geometric phase known as the Aharonov-Casher phase[17], which is analogous to the Aharonov-Bohm phase accumulated via a charge particles in the external magnetic field. This phenomenon referred to as the Aharonov-Casher effect, which provides an effective way to electrically control the magnon propagation[18]. The Aharonov-Casher effect of the magnon has been experimentally observed in a single-crystal yttrium iron garnet[19]. It has been shown that magnons hopping in the time-dependent oscillating electric field can cause some interesting characteristics. Very recently, Owerre has found that hopping magnons in the background of a time-dependent oscillating electric field can generate the Floquet topological magnon insulator, which is analogous to electronic Floquet topological insulator[20,22]. In his works, the ferromagnets on the kagomé, honeycomb ferromagnet, and Lieb lattices have been considered. He has shown that, in Floquet magnon topological insulators, a synthetic or tunable DM interaction can be induced via a circular-polarized laser.

In this paper, we will theoretically study laser-irradiated Floquet topological magnon insulators on a ferromagnetic checkerboard lattice and the corresponding topological phase transition by means of the Floquet-Bloch theory. Our idea is to make use of a circular-polarized laser to induce tunable parameters in checkerboard Floquet topological magnon insulators, which may cause a topological phase transition. By the use of the Floquet-Bloch formalism, we will display that Floquet topological magnon insulators can be transformed from one topological magnon insulator into another one, which has various Berry curvatures, and Chern numbers. Especially, edge states in the checkerboard Floquet topological magnon insulator are also investigated. More details will be presented in the following sections.

## 2. Ferromagnetic checkerboard lattice model

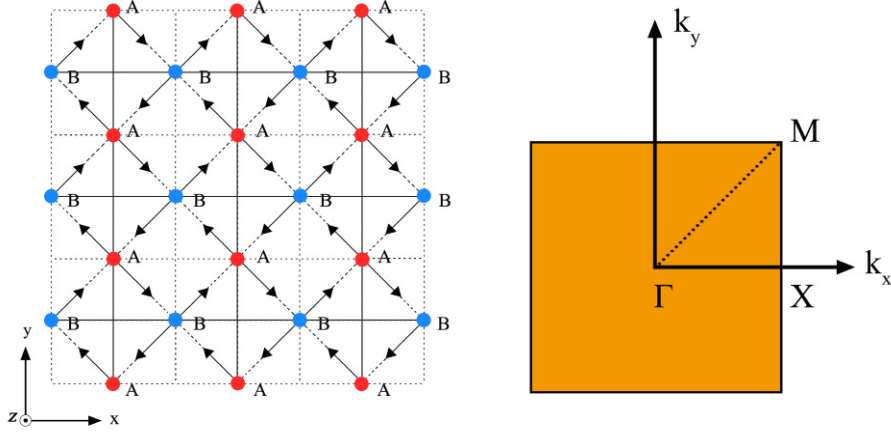


**Fig. 1.** The checkerboard lattice (left) and the corresponding first Brillouin zone (right). We have near neighbor interactions  $J_1$  and  $D$  between spins at site A and site B, and next near neighbor interaction  $J_2$  between site A and A, and B and B, with  $J_2$  along the solid line. Sign of  $\nu_{ij}$  is assumed to be positive when the coupling is along the arrow directions and otherwise negative. In the first Brillouin zone, there exists a path marked connecting the  $\Gamma$ , X, and M points, where  $\Gamma = (0,0)$ ,  $X = (\pi,0)$ , and  $M = (\pi,\pi)$ .

In this work, we consider a Heisenberg ferromagnet on a two-dimensional checkerboard lattice. In principle, the checkerboard lattice can be viewed as a two-dimensional analog of the three dimensional pyrochlore lattice. In the presence of an external field, the Hamiltonian of our checkerboard ferromagnet is given by

$$H = -J_1 \sum_{\langle i,j \rangle} \vec{S}_i \cdot \vec{S}_j - J_2 \sum_{\langle\langle i,j \rangle\rangle} \vec{S}_i \cdot \vec{S}_j + \sum_{\langle i,j \rangle} \vec{D}_{ij} \cdot (\vec{S}_i \times \vec{S}_j) - g\mu_B \vec{H} \cdot \sum_i \vec{S}_i, \quad (1)$$

in terms of the spin operators  $\vec{S}_i$ . The first two terms in the above equation stand for nearest-neighbor and next-nearest-neighbor ferromagnetic Heisenberg interactions ( $J_1 > 0$  and  $J_2 > 0$ ), respectively. The fourth term represents the NN Dzyaloshinskii-Moriya interaction, where  $\vec{D}_{ij}$  is the DMI vector between sites  $i$  and  $j$ . In the light of Moriya's rules, one can assume  $\vec{D}_{ij} = \nu_{ij} D \vec{e}_z$ , where  $\nu_{ij}$  is an

orientation-dependent constant. The last term corresponds to a Zeeman coupling with an external magnetic field  $\vec{H} = H_z \vec{e}_z$ , where  $g$  is the g-factor and  $\mu_B = e\hbar/2m_e$  is the Bohr magneton. As shown in Fig. 1, there are two inequivalent sites A and B in the ferromagnetic checkerboard lattice. Here, there are the ferromagnetic Heisenberg interaction  $J_1$  and the Dzyaloshinskii-Moriya interaction  $D$  between near neighbor spins at sites A and B. Moreover, the ferromagnetic Heisenberg interaction  $J_2$  exist between next near neighbor sites A and A, and B and B.

In order to bosonize the Heisenberg Hamiltonian, we need to employ the Holstein-Primakoff (HP) transformation. Truncated to zeroth order, the HP transformation can be written as  $S^z = S - a^+ a$ ,  $S^+ \approx \sqrt{2S} a = (S^-)^+$ , where  $a^+$  ( $a$ ) corresponds to the magnon creation (annihilation) operator, and  $S^\pm = S^x \pm iS^y$  stand for the spin raising and lowering operators. Substituting the zeroth order HP transformation into Eq. (1), one can obtain the following bosonic hopping Hamiltonian

$$H = f_0 \sum_i (a_i^+ a_i + b_i^+ b_i) - f_1 \sum_{\langle i,j \rangle} (a_i^+ b_j e^{i\varphi_{ij}} + \text{H.c.}) - f_2 \sum_{\langle\langle i,j \rangle\rangle} (a_i^+ a_j + b_i^+ b_j + \text{H.c.}) \quad (2)$$

with  $f_0 = 4J_1 S + 2J_2 S + g\mu_B H$ ,  $f_1 = S\sqrt{J_1^2 + D^2}$ , and  $f_2 = J_2 S$ . The phase

$\varphi_{ij} = v_{ij}\varphi = v_{ij}\arctan\left(\frac{D}{J_1}\right)$  is the fictitious magnetic flux in each unit square plaquette of

the checkerboard lattice. After performing the Fourier transformation, we can obtain

the magnon Hamiltonian in momentum space as  $H(\vec{k}) = f_2 I_{2 \times 2} - \Lambda(\vec{k})$ , where

$\Lambda(\vec{k})$  reads

$$\Lambda(\vec{k}) = \begin{pmatrix} 2f_2 \cos(k_y) & 2f_1 \left[ \cos\left(\frac{k_x + k_y}{2}\right) e^{-i\varphi} + \cos\left(\frac{k_x - k_y}{2}\right) e^{i\varphi} \right] \\ 2f_1 \left[ \cos\left(\frac{k_x + k_y}{2}\right) e^{i\varphi} + \cos\left(\frac{k_x - k_y}{2}\right) e^{-i\varphi} \right] & 2f_2 \cos(k_x) \end{pmatrix}$$

(3)

with  $k_i = \vec{k} \cdot \vec{b}_i$ . Here,  $\vec{b}_1 = (0,1)$  and  $\vec{b}_2 = (1,0)$  are the primitive vectors of the checkerboard lattice in Fig. 1. A straightforward diagonalization of the Hamiltonian  $H(\vec{k})$  yields the energy spectrum of the single magnon, which contains two bands: the upper and lower bands with the dispersion

$$\varepsilon_{\vec{k}}^{\pm} = f_0 - f_2 t_0 \pm \sqrt{t_1 f_1^2 + t_2 f_2^2} \quad (4)$$

with

$$\begin{aligned} t_0 &= \cos(k_x) + \cos(k_y), \\ t_1 &= 4 \left[ 1 + \cos(k_x) \cos(k_y) + \cos(k_x) + \cos(k_y) \cos(2\varphi) \right], \\ t_2 &= \cos(k_x) - \cos(k_y). \end{aligned} \quad (5)$$

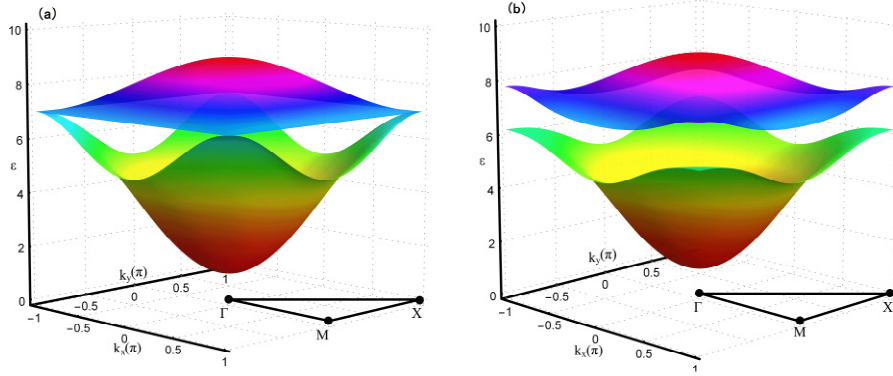


**Fig. 2.** (Color online) The magnon energy bands of the checkerboard ferromagnet: (a)  $D=0$ , (b)  $D=0.2$ . The other parameters are as follows:  $J_1=1$ ,  $J_2=0.5$ ,  $S=1$ ,  $H_z=1$ ,  $g=1$ , and  $\mu_B=1$ .

In Fig. 2, we show the complete magnon energy dispersion relation of the present checkerboard ferromagnet. It is obvious that the magnon energy spectrum comprises two bands: the optical ‘‘up’’ and acoustic ‘‘down’’ bands. When the DM interaction is absent, i.e.,  $D=0$  or  $\varphi=0$ , the optical ‘‘up’’ and acoustic ‘‘down’’ band meet at the X point, as shown in Fig. 2(a). In this case, the checkerboard ferromagnet cannot support the magnon Hall effect. After introducing the DM interaction, the inversion symmetry of the checkerboard lattice is broken

down, which leads to the emergence of a band gap  $\Delta\varepsilon = 8DS$  at the X point as shown in Fig. 2(b). When the band gap opens, the bulk-boundary correspondence can cause the appearance of the topologically protected magnon edge state. Thus, the system becomes a topological magnon insulator. For the checkerboard ferromagnet with the DM interaction, the corresponding Berry curvature, spin Hall conductivity, spin Nernst coefficient, and thermal Hall conductivity have been calculated in Ref.[14].

### 3. Laser-Irradiated checkerboard ferromagnet

#### 3.1. Time-independent Aharonov Casher phase

The concept of driven intrinsic topological magnon insulators has been previously introduced in some quantum ferromagnets. Physically, magnons are regarded as charge-neutral bosonic quasiparticles. Actually, such bosonic quasiparticles are moving magnetic dipoles in ordered magnetic systems. When the quantization of the spin magnetic dipole moment is parallel to the  $z$  direction, the magnetic dipole moment can be represented as  $\vec{\mu} = \mu_m \vec{e}_z$  with  $\mu_m = g\mu_B$ , where  $g$  and  $\mu_B$  stand for the Landé  $g$ -factor and the Bohr magneton, respectively. Here, we suppose that magnons in the insulating quantum checkerboard ferromagnetic system are exposed to an intense laser field with an oscillating electric field  $\vec{E}(\tau)$ , which is irradiated perpendicular to the checkerboard ferromagnet lying on the  $xy$  plane. According to Owerre's idea, then the oscillating electric field  $\vec{E}(\tau)$  can be defined

via  $\vec{E}(\tau) = -\frac{\partial \vec{A}(\tau)}{\partial \tau}$ , where  $\vec{A}(\tau)$  corresponds to the time-dependent vector potential

of the laser field. In the present work, let us consider a laser field with the time-dependent vector potential  $A(\tau) = A_0[\sin(\omega\tau), \sin(\omega\tau + \phi), 0]$ , where  $A_0$  the amplitude of the time-dependent vector potential,  $\omega$  represents the circular frequency of the light, and  $\phi$  is the corresponding phase difference. Obviously, the

vector potential  $\vec{A}(\tau)$  possesses temporal periodicity, i.e.,  $\vec{A}(\tau + T) = \vec{A}(\tau)$ , where  $T = \frac{2\pi}{\omega}$  is the period. In the presence of this time periodic electric field, the magnetic dipole moment of charge-neutral magnon quasi-particles hopping will accumulate the Aharonov Casher phase, namely,

$$\theta_{ij}(\tau) = \frac{g\mu_B}{\hbar c^2} \int_{\vec{r}_i}^{\vec{r}_j} \vec{A}(\tau) \cdot d\vec{l} \quad . \quad (6)$$

The corresponding time-dependent Hamiltonian can be written in the following form

$$\begin{aligned} H(\tau) = & -J_1 \sum_{\langle i,j \rangle} \left[ \frac{1}{2} \left( S_i^+ S_j^- e^{-i\theta_{ij}(\tau)} + S_j^- S_i^+ e^{i\theta_{ij}(\tau)} \right) + S_i^z S_j^z \right] \\ & - J_2 \sum_{\langle\langle i,j \rangle\rangle} \left[ \frac{1}{2} \left( S_i^+ S_j^- e^{-i\theta_{ij}(\tau)} + S_j^- S_i^+ e^{i\theta_{ij}(\tau)} \right) + S_i^z S_j^z \right] \\ & + \frac{iD}{2} \sum_{\langle i,j \rangle} v_{ij} \left( S_j^+ S_i^- e^{-i\theta_{ij}(\tau)} - S_i^- S_j^+ e^{i\theta_{ij}(\tau)} \right) - g\mu_B \vec{H} \cdot \sum_i \vec{S}_i. \end{aligned} \quad (7)$$

It is obvious that the time-dependent Hamiltonian in Eq.(7) has the time periodicity

$$H(\tau + T) = H(\tau) \quad \text{with} \quad T = \frac{2\pi}{\omega} \quad .$$

### 3.2. Floquet-Bloch formalism

In order to investigate the periodically driven quantum system in Eq. (7), we shall make use of the Floquet theory to change this time-dependent model to a static effective model, which is governed via the Floquet Hamiltonian. In principle, the static time-independent effective Hamiltonian  $H_{eff}$  can be expanded in terms of  $\omega^{-1}$ , i.e.,  $H_{eff} = \sum_{m \geq 0} \omega^{-m} H_{eff}^m$ , where  $m$  is integer. One can derive the series expansion of the effective Hamiltonian by means of the discrete Fourier component of the time-dependent Hamiltonian  $H^n = \frac{1}{T} \int_0^T e^{-in\omega\tau} H(\tau) d\tau$ . Thus, we can obtain



$$\begin{aligned}
H^{(n)} = & -J_1 \sum_{\langle i,j \rangle} \left\{ \delta_{n,0} S_i^z S_j^z + \frac{e^{i\frac{\pi}{4}}}{2} \left[ J_n \left( \frac{\sqrt{2}}{2} A_0 \right) S_i^- S_j^+ + J_{-n} \left( \frac{\sqrt{2}}{2} A_0 \right) S_i^+ S_j^- \right] \right\} \\
& - J_2 \sum_{\langle\langle i,j \rangle\rangle} \left\{ \delta_{n,0} S_i^z S_j^z + \frac{e^{i\frac{\pi}{4}}}{2} \left[ J_n (A_0) S_i^- S_j^+ + J_{-n} (A_0) S_i^+ S_j^- \right] \right\} \\
& + iD \sum_{\langle i,j \rangle} v_{ij} \frac{e^{i\frac{\pi}{4}}}{2} \left[ J_{-n} \left( \frac{\sqrt{2}}{2} A_0 \right) S_i^+ S_j^- - J_n \left( \frac{\sqrt{2}}{2} A_0 \right) S_i^- S_j^+ \right] - g\mu_B \vec{H} \cdot \sum_i \vec{S}_i,
\end{aligned} \tag{8}$$

where  $J_n$  is the Bessel function of order  $n \in \mathbb{Z}$ ,  $\frac{g\mu_B}{\hbar c^2}$  has been absorbed in  $A_0$ , and  $\delta_{n,\ell} = 1$  for  $n = \ell$  and zero otherwise.  $J_n(x)$ . In the above derivation, the mathematical relationship  $e^{[iz\sin(x)]} = \sum_{m=-\infty}^{\infty} J_m(z) e^{imx}$  has been used.

For analytical convenience, let us focus on the magnonic Floquet Hamiltonian in the off-resonant regime. When the magnon bandwidth  $\Delta$  of the undriven system is much less than the driving frequency  $\omega$ , namely,  $\Delta \ll \omega$ , this treatment is reasonable. In the off-resonant regime, it suffices to consider the zeroth order of the total effective Floquet Hamiltonian. Thus, we have

$$\begin{aligned}
H_{eff} \approx & - \sum_{\langle i,j \rangle} \left[ J_{1,\perp} (S_i^- S_j^+ + S_i^+ S_j^-) + J_1 S_i^z S_j^z \right] - \sum_{\langle\langle i,j \rangle\rangle} \left[ J_{2,\perp} (S_i^- S_j^+ + S_i^+ S_j^-) + J_2 S_i^z S_j^z \right] \\
& + iD_F \sum_{\langle i,j \rangle} v_{ij} (S_i^+ S_j^- - S_i^- S_j^+) - g\mu_B \vec{H} \cdot \sum_i \vec{S}_i,
\end{aligned} \tag{9}$$

where  $J_{1,\perp} = \frac{1}{2} J_0 \left( \frac{\sqrt{2}}{2} A_0 \right) J_1$ ,  $J_{2,\perp} = \frac{1}{2} J_0 (A_0) J_2$ , and  $D_F = J_0 \left( \frac{\sqrt{2}}{2} A_0 \right) \frac{D}{2}$ . The corresponding time-independent Floquet magnon Hamiltonian is given by

$$H_{eff}(\vec{k}) = f_2 I_{2 \times 2} - \Lambda'(\vec{k}) \tag{10}$$

with

$$\Lambda'(\vec{k}) = \begin{pmatrix} t_0^{AA} f_2 \cos(k_y) & t_0^{AB} f_1 \left[ \cos\left(\frac{k_x + k_y}{2}\right) e^{-i\varphi} + \cos\left(\frac{k_x - k_y}{2}\right) e^{i\varphi} \right] \\ t_0^{AB} f_1 \left[ \cos\left(\frac{k_x + k_y}{2}\right) e^{i\varphi} + \cos\left(\frac{k_x - k_y}{2}\right) e^{-i\varphi} \right] & t_0^{BB} f_2 \cos(k_x) \end{pmatrix}, \tag{11}$$

where

$$t_0^{AA} = 2J_0(A_0), \quad t_0^{AB} = 2J_0\left(\frac{\sqrt{2}A_0}{2}\right), \quad t_0^{BB} = 2J_0(A_0). \quad (12)$$

Obviously, a direct effect of laser-irradiation is that the magnonic Floquet Hamiltonian (9) is analogous to that of a distorted checkerboard ferromagnet with tunable ferromagnetic Heisenberg and DM interactions. In principle, a Floquet checkerboard topological magnon insulator can be generated due to the existence of the tunable DM interaction. In the following text, we shall analyze some topological aspects of the present model.

### 3.3. Laser-induced topological transitions

In the topological systems, the Berry curvature is an very important quantity. Especially, this quantity is the basis of lots of observables in those topological insulators. In magnonic systems, the nontrivial band topology can appear only when the system reveals a nontrivial gap between two magnon energy bands and a nonzero Chern number suggests the presence of magnon edge states in the system. In order to investigate the photoinduced topological phase transitions in the periodically driven topological magnon insulators, the Berry curvature for a given magnon band  $\beta$  ( $\beta = +, -$ ) can be defined as

$$\Omega_\beta(\vec{k}) = - \sum_{\beta' \neq \beta} \frac{2\text{Im}\left(\langle \psi_{\vec{k},\beta}^- | \hat{v}_x | \psi_{\vec{k},\beta'}^- \rangle \langle \psi_{\vec{k},\beta'}^- | \hat{v}_y | \psi_{\vec{k},\beta}^- \rangle\right)}{\left(\varepsilon_{\vec{k},\beta}^- - \varepsilon_{\vec{k},\beta'}^-\right)^2}, \quad (13)$$

where  $\hat{v}_i = \partial H_{\text{eff}}(\vec{k}) / \partial k_i$  ( $i = x, y$ ) stands for the velocity operator,  $\psi_{\vec{k},n}^-$  represents the magnon eigenstate, and  $\varepsilon_{\vec{k},n}^-$  is the corresponding magnon energy eigenvalue.

Furthermore, the linked Chern number can be expressed as a integration with regard to the Berry curvature over the whole first Brillouin zone (BZ), which has the following form

$$C_\beta = \frac{1}{2\pi} \int_{\text{BZ}} d^2k \Omega_\beta(\vec{k}). \quad (14)$$

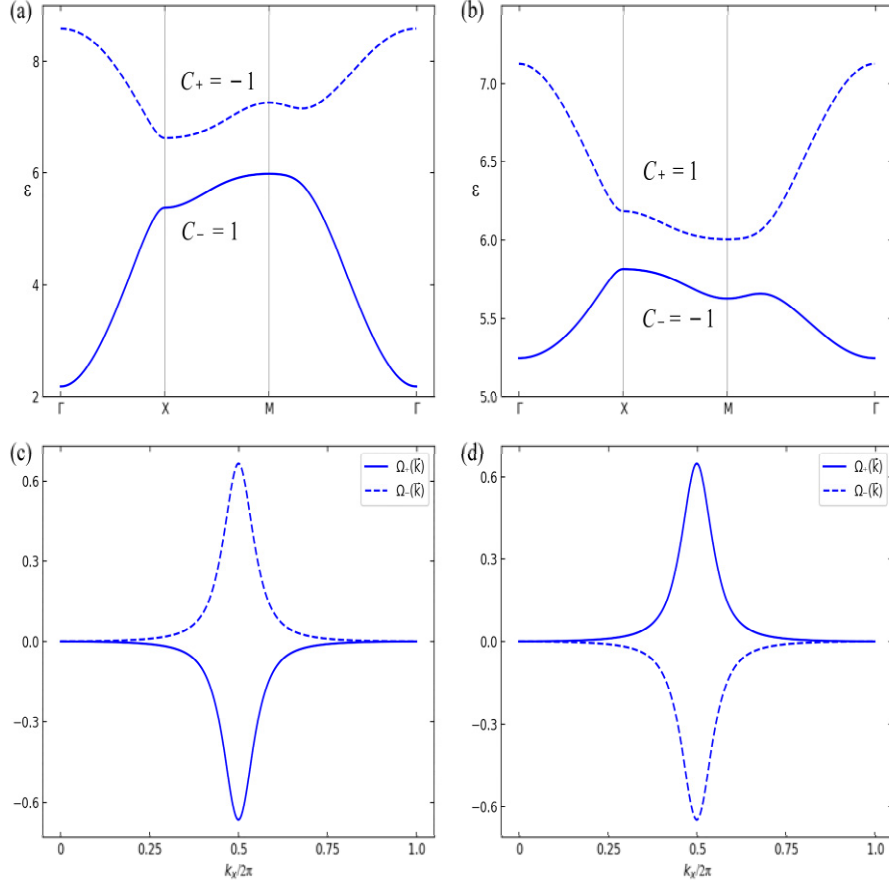


**Fig. 3.** (Color online) Topological magnon bands for the Floquet checkerboard topological magnon insulator (top panel): (a)  $A_0 = 1.3$ , (b)  $A_0 = 2.8$ . Tunable Berry curvatures for the Floquet checkerboard topological magnon insulator at  $k_y = 0$  (bottom panel): (c)  $A_0 = 1.3$ , (d)  $A_0 = 2.8$ . The relevant parameters are set to  $J_1 = 1$ ,  $J_2 = 0.5$ ,  $D = 0.2$ ,  $S = 1$ ,  $H_z = 1$ ,  $g = 1$ , and  $\mu_B = 1$ .

In Fig. 3, we display the Floquet topological magnon bands and the Berry curvatures of the periodically driven checkerboard topological magnon insulator for different light intensities (i.e., different values of  $A_0$ ). It is clearly seen that the acoustic and optical Floquet topological magnon bands and their corresponding Berry curvatures vary as the light intensity changes. Furthermore, Fig. 4 shows the Chern number for the Floquet topological magnon band as a function of the vector potential amplitude  $A_0$ . It is obvious that the topological magnonic system can be switched from one checkerboard Floquet topological magnon insulator with Chern numbers

$(C_+, C_-) = (-1, 1)$  to another one with Chern numbers  $(C_+, C_-) = (1, -1)$ . In fact, these results indicate that varying light intensity field can redistribute the magnon energy band structures of a checkerboard Floquet topological magnon insulator and subsequently leads to a topological phase transition from one checkerboard Floquet topological magnon insulator to another one with different Berry curvatures and Chern numbers.

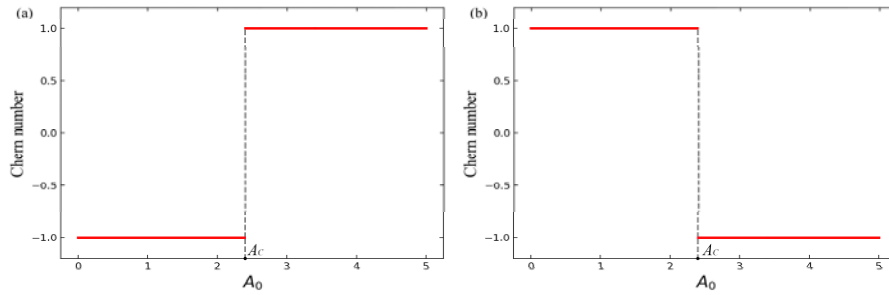


**Fig. 4.** The Chern number for the Floquet topological magnon band as a function of  $A_0$ : (a) the optical “up” band, (b) the acoustic “down” band. Here, the critical value  $A_c$  is approximately equal to 2.40. The other parameters are the same as in Fig. 3.

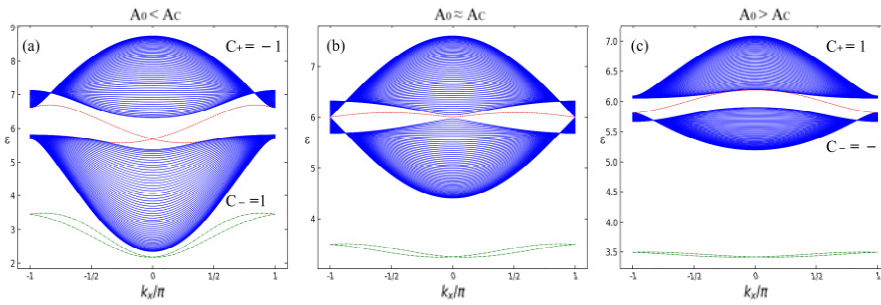


**Fig. 5.** Floquet magnon energy dispersions of edge and bulk states in the laser-irradiated checkerboard ferromagnet with a zig-zag strip geometry at several values of  $A_0$ . The other parameters are the same as in Fig. 3.

Physically, magnon edge states can exist due to the nontrivial topology of the Berry curvatures. Here, let us consider a zigzag boundary. By use of the numerical diagonalization technique, we can calculate the Floquet magnon energy spectrums of a zigzag checkerboard ferromagnet at different light intensities, as shown in Fig. 5.

Under the circularly polarized laser field with high enough frequency, the zeroth order of the total effective Floquet Hamiltonian yields  $H_{DM}^{eff} = D_F \sum_{\langle i,j \rangle} \vec{e}_z \cdot (\vec{S}_i \times \vec{S}_j)$ . Evidently, the intensity of the intrinsic DM interaction can be manipulated via changing the value of  $A_0$ . In the case of  $A_0 < A_c \approx 2.40$  an energy gap appears the X point and it closes in the vicinity of the first zero of the Bessel function  $A_0 \approx A_c$  and reopens for the case of  $A_0 > A_c$ . In Fig. 5, we can see clearly that the topologically protected chiral magnon edge state can appear within the bulk band gap in the case of  $A_0 < A_c$  or  $A_0 > A_c$ . Furthermore, we note that there always exists Tamm-like edge states below the lower band. However, they correspond to topologically trivial edge modes, which are not of interest in the present work.

### 3.4. Laser-induced magnon thermal Hall effects

A crucial consequence of Floquet topological magnon insulators is the Floquet magnon thermal Hall effect. Theoretically, the Floquet magnon edge states causes a transverse heat current when a longitudinal temperature gradient exists. This Floquet magnon edge current can lead to the Floquet magnon thermal Hall effect. The thermal Hall conductivity is an important physical quantity to describe the Floquet magnon thermal Hall effect. Similar to the Hall conductivity in those electronic systems, the thermal Hall conductivity is in connection with the Berry curvature of the Floquet magnon eigenstates. If we only consider the regime in which the Bose distribution function tends to equilibrium, in the nonequilibrium magnonic Floquet system, then the same physical conception of undriven magnon thermal Hall effect can be extended to the laser-induced Floquet topological magnonic system. Thus, the transverse component  $\kappa_{xy}$  of the Floquet thermal Hall conductivity can be written as[20]

$$\kappa_{xy}^F = -k_B^2 T \int_{BZ} \frac{dk^2}{(2\pi)^2} \sum_{\beta=\pm} c_2(n_\beta) \Omega_\beta(\vec{k}) \quad (15)$$

where  $n_\beta = n[\varepsilon_\beta(\vec{k})] = \left( e^{\varepsilon_\beta(\vec{k})/k_B T} - 1 \right)^{-1}$  is the Bose distribution function tending to thermal equilibrium,  $k_B$  stands for the Boltzmann constant,  $T$  corresponds to the absolute temperature, and  $c_2(x) = (1+x) \left( \ln \frac{1+x}{x} \right)^2 - (\ln x)^2 - 2\text{Li}_2(-x)$  with  $\text{Li}_2(x)$  denoting the dilogarithm. Obviously, the Floquet thermal Hall conductivity is considered to be the Berry curvature weighed via the  $c_2$  function. Therefore, any variation in the Berry curvature will influence the Floquet thermal Hall conductivity. In Fig. 6, one can see that the two photoinduced phases in the Floquet topological magnon insulator possess different signs of the Floquet thermal Hall conductivity since the sign of the Berry curvatures varies. Furthermore, we note that the sign of  $\kappa_{xy}^F$  agrees with the sign of the Berry curvature or Chern number of the optical “up” band at low temperatures.

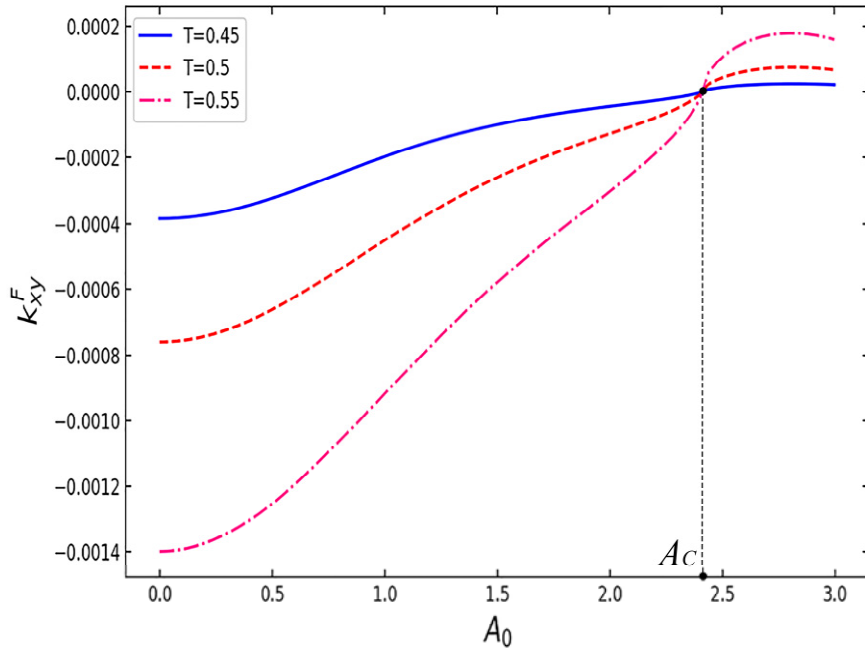


**Fig. 6.** The Floquet thermal Hall conductivity  $\kappa_{xy}^F$  as a function of  $A_0$  for different temperature values. Here, the Boltzmann constant is fixed as  $k_B = 1$ , and the other parameters are the same as in Fig. 3.

#### 4. Conclusions

In summary, we have theoretically a theoretical study on laser-irradiated Floquet topological magnon insulators on a ferromagnetic checkerboard lattice and the corresponding topological phase transition with the help of the Floquet-Bloch theory. It was shown that a Floquet checkerboard topological magnon insulator can be generated on account of the occurrence of the tunable DM interaction induced by a circular-polarized laser. Our results displayed that Floquet checkerboard topological magnon insulators can be transformed from one topological magnon insulator into another one with various Berry curvatures and Chern numbers. Physically, magnon edge states can appear owing to the nontrivial topology of the Berry curvatures. We found that both topologically protected and Tamm-like edge states can appear in the magnon band structure. In addition, we showed that the sign of the Floquet thermal Hall conductivity agrees with the sign of the Berry curvature or Chern number of the optical “up” band at low temperatures.

#### Acknowledgments

This work was supported by the National Natural Science Foundation of China under Grant No. 12064011, the Scientific Research Foundation of Hunan Provincial Education Department under Grant No. 18C0844, the Natural Science Fund Project of Hunan Province under Grant No. 2020JJ4498 and the Graduate Research Innovation Foundation of Jishou University under Grant No. JGY202029.

#### References

- [1] X. L. Qi, S. C. Zhang, *Rev. Mod. Phys.* **83** (2011) 1057-1110.
- [2] A. H. C. Neto, F. Guinea, N. M. R. Peres, K. S. Novoselov, A. K. Geim, *Rev. Mod. Phys.* **81** (2009) 109-162.
- [3] Z. Yang, F. Gao, X. Shi, X. Lin, Z. Gao, Y. Chong, B. Zhang, *Phys. Rev. Lett.* **114** (2015) 114301.
- [4] F. D. M. Haldane, S. Raghu, *Phys. Rev. Lett.* **100** (2008) 013904.

- [5] A. V. Chumak, V. I. Vasyuchka, A. A. Serga, B. Hillebrands, *Nat. Phys.* **11**(2015) 453-461.
- [6] Y. Onose, T. Ideue, H. Katsura, Y. Shiomi, N. Nagaosa, Y. Tokura, *Science* **329** (2010) 297-299.
- [7] R. Matsumoto, S. Murakami, *Phys. Rev. Lett.* **106** (2011) 197202.
- [8] R. Matsumoto, S. Murakami, *Phys. Rev. B* **84** (2011) 184406.
- [9] L. Zhang, J. Ren, J. S. Wang, B. Li., *Phys. Rev. B* **87** (2013) 144101.
- [10] R. Chisnell, J. S. Helton, D. E. Freedman, D. K. Singh, R. I. Bewley, D. G. Nocera, Y. S. Lee, *Phys. Rev. Lett.* **115** (2015)147201.
- [11] S. A. Owerre, *J. Phys.: Condens. Matter* **28** (2016) 386001.
- [12] X. Cao, K.Chen, D. He, *J. Phys.: Condens. Matter* **27** (2015) 166003.
- [13] S. A. Owerre, *J. Phys.: Condens. Matter* **29** (2017) 185801.
- [14] A. S. T. Pires, *Physica B*, **602** (2020) 412490.
- [15] M. Malki,G. S. Uhrig *Phys. Rev. Lett.* **99** (2019) 174412.
- [16] F. Meier, D. Loss, *Phys. Rev. Lett.* **90** (2003) 167204.
- [17] Y. Aharonov, A. Casher, *Phys. Rev. Lett.* **53** (1984) 319-321.
- [18] A. V. Chumak, A. A. Serga, B. Hillebrands, *Nat. Commun.* **5** (2014) 4700.
- [19] X. Zhang, T. Liu, M. E. Flatté, H. X. Tang, *Phys. Rev. Lett.* **113**(2014) 037202.
- [20] S. A. Owerre, *J. Phys. Commun.* **1** (2017) 021002.
- [21] S. A. Owerre, P Mellado, G Baskaran, *Europhys. Lett.***126** (2019) 27002.
- [22] S. A. Owerre, *Sci. Rep.* **8** (2018) 4431.